

# Remote Health Coaching System and Human Motion Data Analysis for Physical Therapy with Microsoft Kinect

Qifei Wang & Gregorij Kurillo  
University of California, Berkeley  
Berkeley, CA 94720, USA

{qifei.wang, gregorij}@eecs.berkeley.edu

Ferda Ofli  
Qatar Computing Research Institute  
Doha, Qatar

fofli@qf.org.qa

Ruzena Bajcsy  
University of California, Berkeley  
Berkeley, CA 94720, USA

bajcsy@eecs.berkeley.edu \*

## Abstract

*This paper summarizes the recent progress we have made for the computer vision technologies in physical therapy with the accessible and affordable devices. We first introduce the remote health coaching system we build with Microsoft Kinect. Since the motion data captured by Kinect is noisy, we investigate the data accuracy of Kinect with respect to the high accuracy motion capture system. We also propose an outlier data removal algorithm based on the data distribution. In order to generate the kinematic parameter from the noisy data captured by Kinect, we propose a kinematic filtering algorithm based on Unscented Kalman Filter and the kinematic model of human skeleton. The proposed algorithm can obtain smooth kinematic parameter with reduced noise compared to the kinematic parameter generated from the raw motion data from Kinect.*

## 1. Introduction

In the last decade, we witness increasing interests for remote monitoring technologies in health care. Remote monitoring captures the activity and other anthropometric data from the subjects. It can perform online analysis of these data, provide health-care feedback to the subjects monitored, and also represent the data to the doctor for further analysis. One typical application is in the physical therapy, especially for the elderly subjects, the doctors need to monitor the subjects physical performance at home during the training sessions and provide further treatments based on the subjects performance.

\*This research was supported by the National Science Foundation (NSF) under Grant No. 1111965.

Human performance capture systems have been widely studied and applied in many applications. However, traditional motion capture systems require particular system setup and markers attached to the subjects monitored which make it impractical for recording motion data at home. Other motion sensors, like the inertia sensors are sensitive to the noise make them also not suitable for motion capture in human daily activities. The emerging accessible and affordable sensing technologies, e.g. the depth sensor, such as Microsoft Kinect, make it possible to capture the humans motion data at home [1].

Recently, we built an interactive exercise coaching system based on Microsoft Kinect [2] intended to encourage elderly adults to perform physical therapy at home. Since this type of sensors were not designed for medical purpose, the acquired motion data are usually noisy with low fidelity for the motion analysis. For example, the joint position data from Microsoft Kinect usually exhibits significant jitters caused by low depth accuracy, occlusions, ambiguity, and loss of tracking. The body segment lengths are also vary during the motion. In order to perform online analysis of subjects performance and feedback to the subjects, we further studied the motion data accuracy from Microsoft Kinect. We also studied the kinematic parameter extraction from the motion data captured by Kinect.

This paper is organized as following: Section 2 introduces the interactive system we have built for the remote physical therapy; Section 3 introduces the work we have done on motion data accuracy evaluation of Microsoft Kinect; Section 4 describes our work on the human kinematic parameters extraction from Kinect motion data; Conclusions are summarized in Section 5.

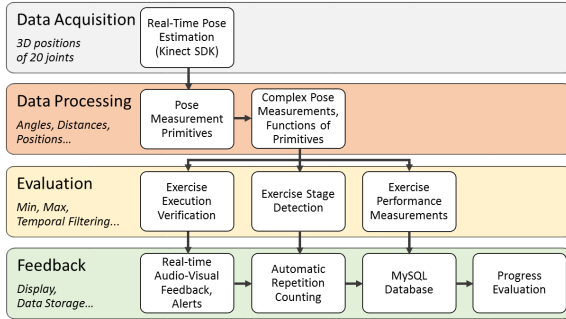


Figure 1. Architecture of our interactive health coaching system.

## 2. Interactive Exercise Coaching System

This system is built for automated exercise coaching of elderly users that would motivate them and track their physical performance when they perform physical therapy at home. The system contains four main modules: data acquisition, data processing, performance evaluation, and feedback. The pipeline of this system is shown in Fig. 1.

In the data acquisition module, we use the Microsoft Kinect camera to record the subjects' motion. Microsoft Kinect captures both the texture and depth information of the scene and provides real-time human skeletal joint data [zhengyou zhang]. Based on the skeletal data estimated by Microsoft Kinect SDK, the data processing module removes outlier data caused by loss tracking with the joint Gaussian and uniform distribution model introduced in Section 3. It further extracts the kinematic parameters from the skeletal motion data. The performance evaluation module does real-time motion analysis, including repetition counting, most moving joints, reachable range, and moving time, which can be further used to measure the flexibilities, endurance, strength, and balance of the subjects. The feedback module can illustrate the evaluation results in the user interface on the screen and also provide both the system automatically generated suggestions and doctors' suggestions to the subject. Moreover, the system stores the subjects' motion data in the database for further reference in the future.

## 3. Kinect Data Accuracy Evaluation

### 3.1. Data accuracy evaluation

In order to quantify the fidelity of the motion data captured by Microsoft Kinect, we evaluated its pose tracking with respect to the motion capture system [5]. In this study, we evaluate both the first and second generations of Microsoft Kinect, which are called Kinect 1 and Kinect 2, respectively, in the following of this section. The motion capture system we use in this evaluation is the PhaseSpace optical motion capture system, which can provide high-precision motion capture data at 120 Hz. The Kinect 1 and

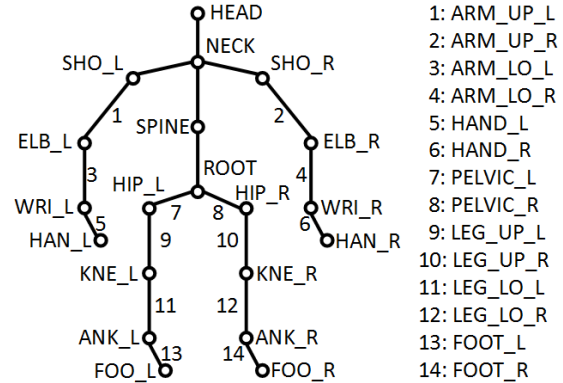


Figure 2. Diagram of the 20-joint skeleton with labeled joint and bone segments that are used in the analysis (L-left, R-right, UP-upper, LO-lower).

Kinect 2 capture the motion data at 20 Hz. During the evaluation, all these three systems capture the human's motion simultaneously. The motion data from these three devices are temporally synchronized using Network Time Protocol (NTP). The skeletal joint data from Kinect 1 and Kinect 2 are extracted based on the latest SDK of them. The skeletal joint data from the motion capture system are obtained by the Recap2 software. We picked 20 common joints and 14 common segments among the three systems. The joints and segments picked in the evaluation are demonstrated in Fig. 2.

During the evaluation, we perform 12 different exercises that six of them are in the sitting pose, which are designed by the physical therapist for the elderly people with physical problems. The other six are in the standing pose, which is the most common motion that people may perform in their daily lives. Each exercise is performed by the subjects for five times and captured in three different view angles, including the frontal view, right side view with 30 degree and 60 degree. The degree here means the angle between the subjects' frontal direction and the optical axis of the Kinect cameras.

For the joint position, we evaluate the offset and variance of the joint positions obtained by Kinect 1 and Kinect 2 with respect to the corresponding joint position captured by the motion capture system. All the joint positions from these three systems are transformed into a unified coordinate system by the camera calibration performed before the motion capture.

Tables 1 and 2 show the average joint offset and variance of the offset in the sitting and standing exercise, respectively.

We also evaluate the segment length based on the motion data. Tables 3 and 4 demonstrate the average segment length error and variance of the segment length in the sitting

Table 1. Joint position offsets in sitting exercises.

	Kinect 1						Kinect 2					
	Mean (mm)			SD (mm)			Mean (mm)			SD (mm)		
	0°	30°	60°	0°	30°	60°	0°	30°	60°	0°	30°	60°
ROOT	256	262	263	25	20	25	100	102	106	17	18	16
SPINE	91	97	100	24	20	21	110	117	126	13	14	11
NECK	79	65	62	25	21	23	84	78	73	14	16	14
HEAD	74	70	67	26	21	21	50	51	50	13	15	12
SHO_L	90	89	97	26	24	33	76	76	82	16	24	29
ELB_L	81	86	98	27	29	35	87	103	114	17	28	25
WRI_L	76	90	118	33	48	55	59	84	115	25	53	44
HAN_L	85	106	134	41	60	68	64	95	125	31	60	53
SHO_R	78	74	69	28	24	23	80	83	78	17	20	17
ELB_R	95	93	89	28	38	34	88	77	70	21	25	19
WRI_R	64	93	110	30	53	65	61	64	71	25	28	24
HAN_R	83	113	130	35	65	80	74	71	75	24	28	26
HIP_L	188	200	215	25	20	22	115	122	139	16	17	15
KNE_L	96	95	93	24	24	27	76	95	114	16	18	25
ANK_L	54	77	81	17	25	32	93	103	113	16	18	29
FOO_L	66	74	86	19	26	38	93	105	119	18	25	39
HIP_R	207	210	211	25	21	24	133	128	132	15	18	16
KNE_R	123	118	128	23	23	34	120	117	119	15	17	24
ANK_R	67	75	91	17	21	27	112	122	132	15	19	27
FOO_R	67	74	84	17	20	26	126	134	139	19	20	28

Table 2. Joint position offsets in standing exercises.

	Kinect 1						Kinect 2					
	Mean (mm)			SD (mm)			Mean (mm)			SD (mm)		
	0°	30°	60°	0°	30°	60°	0°	30°	60°	0°	30°	60°
ROOT	245	256	267	23	25	25	76	81	93	24	19	18
SPINE*	79	89	102	22	22	24	112	129	144	17	16	17
NECK	82	91	102	23	24	23	113	129	143	18	16	16
HEAD	89	84	87	30	29	26	79	82	90	26	22	20
SHO_L	76	76	80	33	36	38	68	72	78	29	31	31
ELB_L	98	112	134	46	52	66	112	137	159	37	41	57
WRI_L	85	93	110	56	57	71	66	84	111	47	52	73
HAN_L	85	96	114	62	65	80	77	94	121	49	55	80
SHO_R	76	76	74	30	30	26	96	106	109	26	24	22
ELB_R	98	89	80	38	39	34	96	91	80	33	32	31
WRI_R	80	82	80	43	43	38	78	88	87	33	32	31
HAN_R	85	83	77	46	49	44	81	79	74	33	34	32
HIP_L	186	205	228	28	27	27	106	125	150	23	19	21
KNE_L	101	111	124	33	38	52	107	129	148	26	34	51
ANK_L	119	144	135	43	61	58	135	168	174	33	51	58
FOO_L	115	135	122	42	60	59	130	170	180	33	56	63
HIP_R	188	195	207	25	24	23	103	104	109	25	17	17
KNE_R	105	102	101	31	29	26	115	119	118	26	25	27
ANK_R	111	113	108	38	39	28	146	158	157	32	33	35
FOO_R	97	93	86	36	37	29	146	157	150	32	33	38

Table 3. Mean and SD of the bone length difference, sitting pose

	Kinect 1						Kinect 2					
	Mean (mm)			SD (mm)			Mean (mm)			SD (mm)		
	0°	30°	60°	0°	30°	60°	0°	30°	60°	0°	30°	60°
ARM_UP_L	-76	-74	-81	17	18	21	-67	-62	-68	14	17	20
ARM_LO_L	-46	-40	-32	17	22	27	-39	-30	-24	14	19	23
HAND_L	-3	-4	-3	22	19	20	-20	-17	-17	20	24	25
ARM_UP_R	-68	-70	-69	17	17	18	-67	-67	-69	15	14	13
ARM_LO_R	-37	-30	-29	17	20	21	-35	-28	-30	13	15	16
HAND_R	2	3	3	21	24	24	-15	-13	-9	20	19	17
PELVIC_L	-28	-28	-36	6	5	8	-54	-62	-75	3	3	4
LEG_UP_L	49	38	38	30	32	34	9	5	5	16	18	18
LEG_LO_L	-90	-100	-81	23	28	31	-80	-79	-75	17	18	21
FOOT_L	-13	-4	1	8	10	13	36	38	32	12	14	19
PELVIC_R	-29	-33	-41	6	5	7	-52	-47	-49	3	3	4
LEG_UP_R	44	46	53	31	28	31	1	9	18	16	18	18
LEG_LO_R	-86	-88	-95	25	26	31	-76	-82	-74	17	19	23
FOOT_R	-8	-2	8	7	9	11	41	44	40	12	11	12

Table 4. Mean and SD of the bone length difference, standing pose

	Kinect 1						Kinect 2					
	Mean (mm)			SD (mm)			Mean (mm)			SD (mm)		
	0°	30°	60°	0°	30°	60°	0°	30°	60°	0°	30°	60°
ARM_UP_L	-60	-62	-65	19	22	23	-54	-54	-51	15	18	20
ARM_LO_L	-30	-31	-34	16	18	20	-34	-33	-32	17	17	18
HAND_L	-7	-5	0	21	21	23	-32	-32	-27	20	21	23
ARM_UP_R	-53	-58	-59	21	19	18	-59	-66	-66	17	14	14
ARM_LO_R	-22	-22	-22	17	18	20	-30	-27	-25	18	18	17
HAND_R	-1	4	6	23	21	19	-21	-16	-14	19	18	18
PELVIC_L	-27	-30	-37	9	7	8	-52	-63	-75	5	5	5
LEG_UP_L	113	119	137	28	33	39	-13	-10	4	19	21	25
LEG_LO_L	-64	-66	-65	29	29	31	-79	-85	-86	21	23	25
FOOT_L	-6	-1	2	9	12	12	43	42	34	9	12	14
PELVIC_R	-28	-34	-41	7	6	8	-47	-44	-44	7	4	5
LEG_UP_R	103	115	128	29	27	29	-25	-18	-6	18	18	20
LEG_LO_R	-61	-57	-58	26	25	25	-79	-79	-77	20	20	20
FOOT_R	-2	1	4	8	9	10	48	45	32	9	11	16

and standing exercises.

The results shows that overall Microsoft Kinect 2 generates more stable skeletal joint tracking with less offset and variance as compared to Microsoft Kinect 1. The variance of the joint position and segment length are both increasing with the view angle increasing. Some joints usually have larger offset and variance than the other joints, e.g. the hip and knee joints in Kinect 1, the ankle and foot joints in Kinect 2.

### 3.2. Outlier data removal

The joint position offsets and variance in general depend on various sources of error, such as systematic errors,

noise from depth quantization, occlusions, and ambiguity, etc. Compared to the multi-view motion capture system, the Kinect camera captures the motion data from a single view-point [7]. The occlusions and ambiguity from a single view-point will cause loss of tracking. Although the Kinect can infer the joint position based on the related body part [3], it is not reasonable to perform motion data analysis based on the inferred motion data due to tracking loss. Therefore, we analyze the error distribution to discriminate between the random errors and the errors due to tracking loss.

Generally, the random systematic errors follow the Gaussian distribution while the errors due to tracking loss can

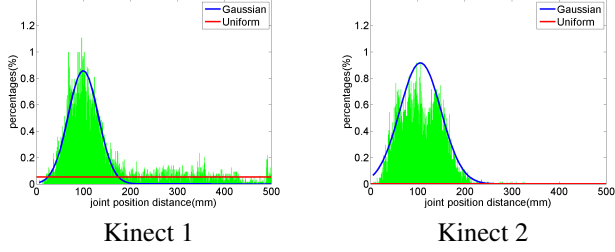


Figure 3. Mixture model fitting into the distribution of joint position offsets for the right elbow (viewpoint:  $60^\circ$ ).

be treated as outliers belonging to a uniform distribution. Therefore, we use a mixture model of a Gaussian distribution and a uniform distribution to approximate the distribution of the joint position offsets, as defined in equation 1.

$$p(\theta) = \rho \times N(\mu, \sigma) + (1 - \rho) \times U(x_1, x_2). \quad (1)$$

In equation 1,  $p$  denote the mixture distribution of joint position,  $\theta$ ,  $N(\mu, \sigma)$  and  $U(x_1, x_2)$  denote the Gaussian and uniform distribution, respectively,  $\rho$  denotes the weighting parameter. Fig. 3 demonstrates the distribution fitting results for the right elbow in the exercise. The results show the mixture model of the Gaussian and uniform distributions overlaid on the data histograms.

By applying the mixture model and maximal likelihood estimation, we can remove the outlier data which satisfy the uniform distribution and make cleaner data for the further analysis. Table I demonstrates the joint offset of both standing and sitting exercises without the outlier data.

Table 5. Average joint position offsets without outliers.

		Mean (%)			SD (%)		
		$0^\circ$	$30^\circ$	$60^\circ$	$0^\circ$	$30^\circ$	$60^\circ$
Kinect 1	Sitting	5	8	6	35	38	35
	Standing	8	7	8	39	36	33
Kinect 2	Sitting	2	5	3	23	36	23
	Standing	8	5	6	49	46	43

## 4. Kinematic parameter estimation

The kinematic parameters, such as the segment length, joint quaternion, and positions are widely used in human motion analysis and human robotic interaction. For the high fidelity motion data, the kinematic parameters can be directly estimated from the skeletal joint position. However, generating the kinematic parameters from the noisy motion data captured by Kinect will propagate the noise into the following processing and analysis steps. In order to reduce the noise in the derived kinematic parameters from the

Kinect noise motion data, we propose a kinematic filtering approach in this section.

### 4.1. Kinematic model

In motion analysis, the humans skeleton can be represented as a series joints which are connected by bones. Therefore, the each joint position can be derived by its parent joint position, the corresponding segment orientation and length. The humans skeleton can thus be represented as a kinematic chain. In this paper, we treat the root joint as the root of each kinematic chain. Based on the skeletal structure shown in Fig. 2, the SPINE, NECK, SHO\_L, SHO\_R, HIP\_L, and HIP\_R are modeled as the 3-DoF joints and their parent joints are ROOT, SPINE, NECK, NECK, ROOT, ROOT, respectively; The ELB\_L, ELB\_R, KNE\_L, KNE\_R are treated as the 1-DoF joints whose parent joints are SHO\_L, SHO\_R, HIP\_L, HIP\_R, respectively; The WRI\_L, WRI\_R, ANK\_L, and ANK\_R are the 2-DoF joints that their parent joints are ELB\_L, ELB\_R, KNE\_L, KNE\_R, respectively. For each joint, its position can be derived by its parent joint position,  $\mathbf{T}_p$ , the segment length of its corresponding segment,  $l_c$ , the relative rotation matrix of its corresponding segment,  $\mathbf{R}_l$ , with respect to its parent segment, the rotation matrix of its parent segment,  $\mathbf{R}_p$ , as the following function  $\mathbf{F}$ :

$$[\mathbf{T}_c, 1]^T = F(\mathbf{T}_p, l_c, \mathbf{R}_l, \mathbf{R}_p) = \begin{bmatrix} \mathbf{R}_l \times \mathbf{R}_p & \mathbf{T}_p \\ 0 & 1 \end{bmatrix} \times \begin{bmatrix} 0 \\ 0 \\ l_c \\ 1 \end{bmatrix} \quad (2)$$

### 4.2. Kinematic filtering

With the kinematic model presented in the last section, we propose a kinematic filtering algorithm based on Kalman filtering to generate the kinematic parameter from the Kinect motion data [6]. The input state vector is constituted by the root joint position, the segment length, and the segment rotation quaternion. The observation vector is constituted by the rest joint positions. The state transition is modeled by a random-walk process. The observation measuring function is a set of the kinematic model function as defined by equation 2. Since the state transition and the observation measuring functions are nonlinear, we apply the Unscented Kalman Filter (UKF) [4] for the filtering. Since the segment lengths for a certain person are constants, we propose a four-pass UKF to meet with this constraints. In the first forward pass, the UKF is defined by the following functions

$$\mathbf{x}(t) = \mathbf{x}(t-1) + \delta(t) \quad (3)$$

$$\mathbf{y}(t) = \mathbf{F}(\mathbf{x}(t)) + \varepsilon(t) \quad (4)$$

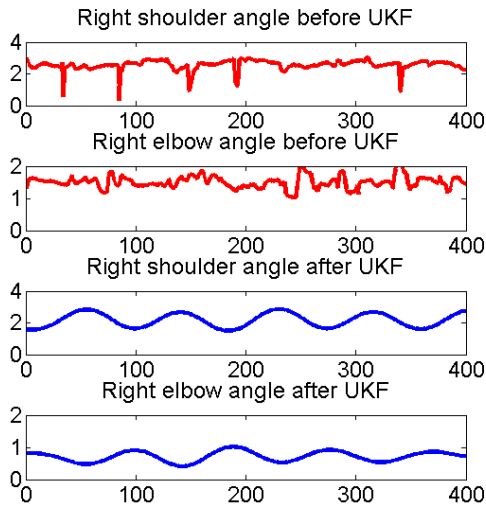


Figure 4. Joint angles of the shoulder and elbow calculated by the input raw motion data and the output kinematic parameters, respectively, horizontal axes represent the frame count, vertical axes represent the joint angle.

In equations 3 and 4, the  $\mathbf{x}(t)$  and  $\mathbf{x}(t + 1)$  denote the state vector at time  $t$  and  $t + 1$ , respectively,  $\delta$  denote the random term in the random walk process,  $\mathbf{y}$  denote the observation vector,  $\varepsilon$  denotes the observation noise. In the first backward pass, the observation measuring function is the same as equation 4. The state transition function is defined as

$$\mathbf{x}(t) = \mathbf{x}(t + 1) + \delta(t) \quad (5)$$

After the first two pass, the length of each segment are assigned as a constant in the following forward and backward passes. The covariance and the random terms in the random walk process of the segment lengths are all set to zeros.

Fig. 4 demonstrates the filtering results of UKF for the motion data from Kinect 1. The segment quaternion curves after filtering are much smoother than the input noisy data and also demonstrate strong periodic pattern which is in accordance to the input motion. Therefore, the UKF based on the kinematic model is a practical solution to extract kinematic parameters.

## 5. Conclusions

This paper summarize the recent progress in the motion analysis for physical therapy with the affordable and accessible device like Microsoft Kinect. Based on preliminary studies, our remote health coaching system receive positive feedback from the users for its accessibility and interaction. Since the motion data captured by Microsoft Kinect is

noisy, we further studied the data fidelity of each joint position and segment length. We also propose a mixture model to distinguish the outlier data caused by loss of tracking. It can helps to reduce the noise in the further motion data analysis. Finally, the kinematic filtering based on UKF provide a solution to extract smooth kinematic parameters from the noisy motion data.

## References

- [1] H. M. Hondori and M. Khademi. A review on technical and clinical impact of microsoft Kinect on physical therapy and rehabilitation. *Journal of Medical Engineering*, 2014:16, 2014.
- [2] F. Ofli, G. Kurillo, S. Obdrzalek, R. Bajcsy, H. Jimison, and M. Pavel. Design and evaluation of an interactive exercise coaching system for older adults: Lessons learned. *IEEE Journal of Biomedical and Health Informatics*, page 15, *Epub ahead of print*. 2015.
- [3] J. Shotton, A. Fitzgibbon, M. Cook, T. Sharp, M. Finocchio, R. Moore, A. Kipman, and A. Blake. Real-time human pose recognition in parts from single depth images. In *Proceedings of IEEE Conference on Computer Vision and Pattern Recognition (CVPR)*, pages 1297–1304, 2011.
- [4] E. Wan, R. Van Der Merwe, et al. The unscented kalman filter for nonlinear estimation. In *Proceedings of IEEE Adaptive Systems for Signal Processing, Communications, and Control Symposium (AS-SPCC)*, pages 153–158, 2000.
- [5] Q. Wang, G. Kurillo, F. Ofli, and R. Bajcsy. Evaluation of pose tracking accuracy in the first and second generations of microsoft kinect. *arXiv preprint arXiv:1512.04134*, 2015.
- [6] Q. Wang, G. Kurillo, F. Ofli, and R. Bajcsy. Unsupervised temporal segmentation of repetitive human actions based on kinematic modeling and frequency analysis. In *International Conference on 3D Vision (3DV)*, pages 562–570, 2015.
- [7] Z. Zhang. Microsoft Kinect sensor and its effect. *MultiMedia, IEEE*, 19(2):4–10, Feb 2012.